Journal of
Materials Chemistry A

Accepted Manuscript

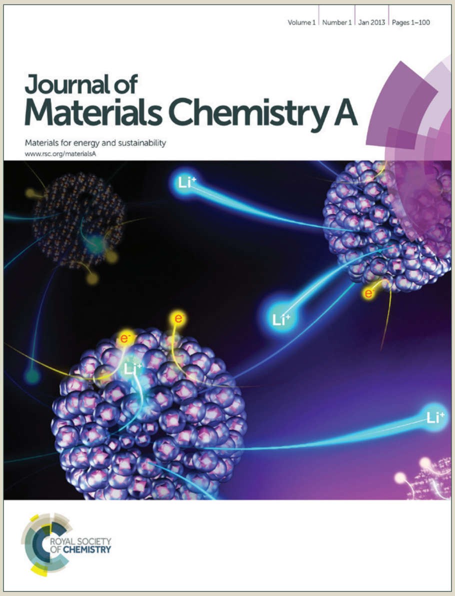

ROYAL SOCIETY
OF **CHEMISTRY**

www.rsc.org/materialsA

Journal Name RSCPublishing

ARTICLE

Template synthesized ultra-thin molecularly imprinted polymers membrane for selective preconcentration of dyes

Lili Lu,[a,b] Xianyang Yue,[b] Fuquan Lin,[a,c] Feng Huang,[b] Bintian Zhang*[c] and Zhang Lin*[c,d]

Selective and efficient removal of pollutants is essential for wastewater treatment and resource recycling. In this study, an ultra-thin molecularly imprinted polymers (MIPs) membrane with a thickness of 1 nm was synthesized by a facile atom transfer radical polymerization (ATRP) method using layered double hydroxides (LDH) as the template substrate. The as-prepared MIPs membrane was characterized by XRD, TEM, AFM, FTIR and BET measurement. This material was then applied for the selective preconcentration of Rhodamine B (RhB) in water. Benefiting from the surface imprinting technique, a high adsorption capacity of 100.1 mg/g was obtained, with an enrichment multiple of 27.3 times. It was interesting that the adsorption of the MIPs was temperature-sensitive, which was employed as a simple and environmental-friendly desorption strategy by changing the operating temperature. Applicability of the material was demonstrated by recovering RhB from real water samples. This membrane-structure MIPs are highly selective, reproductive, and can be large-scale produced, and thus is a promising adsorbent for the treatment of wastewater and recycling of organic resources.

1 Introduction

Dyes are widely used in industries such as textiles, rubber, plastics, paper-making and so on[1]. Over 7 × 10^5 tons of about 10000 different commercial dyes and pigments are produced and used annually all over the world. Most of them are consumed by textile industries. It has been estimated that 10-15% of the dyes are lost during the dyeing process and released with the sewage[2], resulting in serious water pollution. As we known, dye wastewater is toxic, carcinogenic, mutagenic or teratogenic to various microbiologic and fish species[3], and environmental events caused by dye wastewater have been frequently reported. Thus, it is an urgent task for the treatment of dye wastewater. Traditional technologies for dye wastewater treatment include chemical oxidation, electrochemistry, membrane technology, coagulation, flocculation, biological degradation and adsorption technique[4-10], etc. Among them, adsorption methods have been very popular for their feasibility and cost-effectiveness. However, conventional adsorbents such as activated carbon, natural minerals, and industrial waste residue[10-12], are ineffective in the treatment of low concentration dye wastewater. In addition, as the adsorption by the materials is often non-selective, dyes cannot be recycled and reused after the treatments. In the past two decades, nanomaterials have been regarded as excellent adsorbents. As demonstrated in our previous works, Wang et al.[13, 14] reported efficient removal of anionic and cationic dyes from low concentration dye wastewater by $Mg(OH)_2$ and ZnS@Cu, respectively. However, these adsorbents still fail in the selective adsorption of a certain dye. Therefore, it is significantly essential to develop a material that can satisfy both the requirements of advanced dye wastewater treatment and dyes recycling.

Molecular imprinting, a well-known technology, is used to create specific recognition cavities in synthetic polymers called molecularly imprinted polymers (MIPs). The recognition of MIPs mainly imitates the biological processes such as ligand-receptor binding, substrate-enzyme reactions and translation and transcription of the genetic code[15]. These recognition cavities can be tailor-made according to different demands, hence exhibiting excellent affinity and selectivity towards imprinted molecules. Furthermore, MIPs also possess the advantages of low cost and easy preparation, good chemical and physical stability, and stable reusability[16]. MIPs have been employed in many fields, such as biological and chemical sensor, quantitative detection, separation and purification and so on[17-22]. Although the MIPs prepared by bulk polymerization provide adequate selectivity, there are still some shortcomings including time-consuming preparation procedure, low-affinity binding, high diffusion barrier, low-rate mass transfer, and poor site accessibility[23]. Therefore, this kind of MIPs display low adsorption amount and poor treatment effect to target molecules so that their application in treating wastewater is restricted. As alternatives, some researchers synthesized micro-spheres or micro-particles structure MIPs to treat water pollutants[1, 24-26]. The preparation processes have been actually simplified and the adsorption amount has been improved to some degree, but the treatment effect is still unsatisfied. It is well known that membrane-structure imprinted materials have high surface area that a large number of specific recognition sites can be located at or approximate to the surface of materials, which is beneficial for recognition, combination and elution of the template molecules compared with conventional imprinted materials. Recently, surface imprinted polymers modified on substrates, including partially carbon nanotubes[27, 28] silicon wafer[29, 30], organic substrate[31] and porous anodic alumina oxide[32], have been adopted to acquire the membrane-structure imprinted materials. This kind of MIPs exhibit very high adsorption amount and selectivity. However, as the synthesis procedure is very complicated, large-scale production of the materials is impossible, which limits their application in wastewater treatment.

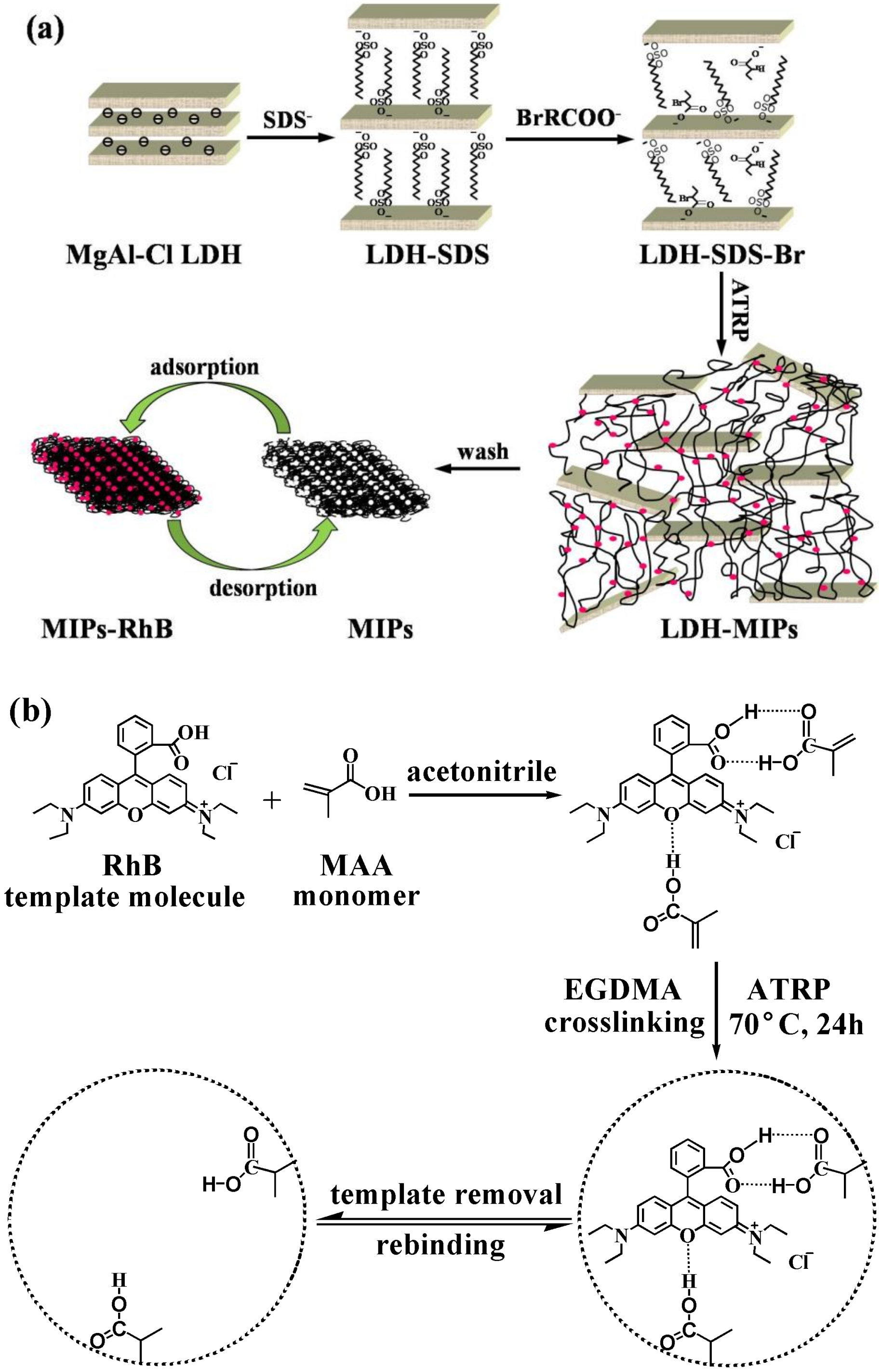

Scheme 1. Scheme for preparation of ultra-thin MIPs membranes and their application (a) and imprinting process of the MIPs for RhB (b).

Layered double hydroxides (LDH) are a kind of two-dimensional structure inorganic materials. The LDH can be mass-produced by a simple and rapid method and removed easily by washing with acid solutions. The structure of LDH is composed of positive charged layers as well as charge complementing anions and solvent molecules in the interlayer. These anions and solvent molecules can be exchanged reversibly with other anions and molecules such as monomers, templates, crosslinker, initiators of polymerization and so on[33]. As a result, LDH is an ideal template matrix for the synthesis of in-situ imprinting polymers. As a controlled radical polymerization, atom transfer radical polymerization (ATRP) has been a popular method to graft polymer brushes because of the wide applicability of monomers, good compatibility of functional groups and excellent controllability for product molecular weight and dispersity[32]. Given the characteristics of LDH and ATRP mentioned above, we hypothesize that conjunction of ATRP technique and

LDH can lead to an efficient method for large-scale synthesis of membrane-structure MIPs.

In this work, we introduce a facile approach for the preparation of membrane-structure MIPs using LDH as the template matrix and ATRP as the polymerization method. The as-prepared MIPs had an ultra-thin membrane-structure of about 1 nm and presented excellent adsorption characteristics and selectivity. This material was then used for the treatment of low concentration dye wastewater. It could be a promising adsorbent for the advanced treatment of wastewater and recycling of resources.

2 Experimental

2.1 Materials

Methylacrylic acid (MAA), ethylene glycol dimethacrylate (EGDMA), 2,2'-dipyridyl (2,2'-bpy), cuprous bromide (CuBr), α-bromobutyric acid, rhodamine 6G (Rh6G) and Butyl rhodamine B (BRhB) were supplied by Aladdin (Shanghai, China). Rhodamine B (RhB), acetonitrile, $MgCl_2$ $6H_2O$, $AlCl_3$ $6H_2O$, methyl alcohol, acetic acid and ammonium hydroxide were obtained from Shanghai Chemical Reagents Co. (Shanghai, China). And sodium lauryl sulfate (SDS) was purchased from Tianjin reagent (Tianjin, China). All reagents were of analytical grade and used without further purification.

2.2 Characterization

X-ray diffraction (XRD) was used to identify the phase and crystal structure of the obtained samples. Diffraction data were recorded using a PANalytical X'Pert PRO diffractometer with Cu Kα radiation (40 kV, 40 mA) in the continuous scanning mode. The 2θ scanning range was from 2° to 13° and 5° to 85° in steps of 0.0167°. The morphology of samples was observed by Transmission electron microscopy (TEM, JEM2010, JEOL, Tokyo, Japan). The elemental analyses were implemented by using an INCA X-ray energy-dispersive spectroscopy (EDS, Oxford Instruments, UK). The thickness of the membrane was measured by Agilent 5500 AFM (Palo Alto, CA, USA). The BET surface area was measured using an ASAP 2020 C+M Micropore analyzer (Micromeritics Instrument Crop., GA). The polymers were degassed at 200 ℃ in vacuum prior to adsorption. IR spectra were recorded on a VERTEX70 FT-IR spectrometer (Bruker Optics, GER), using KBr pellets in the range of 4000~500 cm^{-1}. A Shimadzu UV-2550 spectrophotometer (Tokyo, Japan) was used to record the UV/vis spectra of the samples.

2.3 Preparation of MgAl-Cl LDH

The MgAl-Cl LDH (LDH) was synthesized by a coprecipitation method reported previously by Li et al[34]. In brief, a mixed solution of $MgCl_2$ $6H_2O$ and $AlCl_3$ $6H_2O$ was prepared with an Mg/Al molar ratio of 3:1. Ammonium hydroxide was used to adjust the pH value of the mixed solution by slowly dropping with continuous stirring. The final pH value of the suspension was about 9.5. Then the precipitate was aged for 3 h in solution at room temperature. The obtained product was filtered, washed and dried at 100 ℃ for 24 h.

2.4 Preparation of the ATRP initiator

The initiator of ATRP (LDH-SDS-Br) was synthesized via chemical modification of LDH including the anion exchange reactions with SDS^- and α-bromobutyrate, respectively for two times, as illustrated in scheme 1a. According to literature[35], the chemical modification of LDH was conducted by the anion exchange reaction of 2.0 g of LDH with 100 mL of 0.1 M SDS at 60 ℃ for 2 days, yielding LDH-SDS. Subsequently, the exchange of dodecyl sulfate (SDS^-) for α-bromobutyrate was implemented in ethanol/deionized water (5%, v/v) at 20 ℃ for 3 days, and the product, termed LDH-SDS-Br, was used as the ATRP initiator.

2.5 Preparation of RhB-MIPs and corresponding NIPs

The RhB-MIPs were prepared by an ATRP method, described by Wang et al.[32], using RhB, MAA and EGDMA as the template molecule, functional monomer and crosslinking agent, respectively (Scheme 1b). Firstly, 1.25 mmol of RhB, 10 mmol of MAA and 80 mmol of EGDMA were dissolved in 80 mL of acetonitrile. The solution was mixed by stirring in an ice bath. After 3 h of incubation, the solution was purged with N_2 for 30 min and then transferred to a wolff bottle containing ATRP initiator (1.0 g), organometallic catalysts CuBr (0.38 mmol) and 2,2'-bpy (2.28 mmol). Secondly, this reaction system was sealed and incubated at 70 ℃ under continuous stirring and protection of N_2 for 24 h. The resultant products were collected by centrifuging and washing with ethanol several times to remove the residual monomers and crosslinking agent. Afterwards, the substrate (LDH) and template (RhB) were removed by methanol/acetic acid (9:1, v/v), which was repeated several times until LDH and RhB could not be detected by XRD/EDS and UV/vis spectrophotometer, respectively. Subsequently, the products were rewashed three times with distilled water to remove acid solution. Finally, the polymers were dried at 60 ℃ under vacuum. The corresponding non-imprinted polymers (NIPs) were prepared by the same process, but without the adding of the template molecule (RhB).

2.6 Adsorption experiments

To evaluate the effect of temperature on the adsorption capacity of the material, MIPs (1 mg) were incubated with 0.1 mM RhB solution (2 mL) for 24 h at different temperature (20 ℃, 23 ℃, 25 ℃, 27 ℃, 30 ℃, 35 ℃, and 40 ℃). The static adsorption tests were carried out by incubation of 1 mg of MIPs or NIPs with 4 mL of RhB solution with concentrations ranging from 1 μM to 1 mM at 25 °C. After stirring for 24 h to reach the adsorption equilibrium, the mixture was then centrifuged at 10000 rpm for 3 min and the RhB in the supernatant was determined by UV/vis spectrometer at the wavelength of 554 nm. The amount (Q_e, mg/g) of RhB adsorbed by MIPs or NIPs was calculated referring to the following formula:

$$Q_e = (C_0 - C_e) \cdot M \cdot V/W$$

where C_0 is the initial RhB concentration (mM), C_e is the RhB concentration after adsorption equilibrium (mM), M is the molar mass of RhB (g/mol), V is the volume of RhB solution (mL), and W is the weight of MIPs and NIPs (mg).

The kinetic adsorption test was investigated by mixing of 5 mg MIPs or NIPs in 100 mL of 0.025 mM RhB solution, and then stirring continuously for 36 h at 25 ℃. One millilitre of the mixture was sampled at appropriate time intervals, and centrifuged at 10000 rpm for 3 min to obtain the supernatant. The imprinting ability of the MIPs was estimated by imprinting factor (α), which is defined as in the following formula:

$$\alpha = Q_{MIPs}/Q_{NIPs}$$

where Q_{MIPs} and Q_{NIPs} are the adsorption amount of template molecule by the MIPs and the corresponding NIPs, respectively.

Selectivity of the MIPs was studied using Rh6G and BRhB as the analogues of RhB. A mixture solution was prepared from the three dyes, with an initial concentration of 0.1 mM for each dye. The experiment procedure was similar to that of the static adsorption experiment. The recognition ability of MIPs was assessed by selectivity coefficient (β), which is expressed as in the following formula:

$$\beta = Q_m/Q_n$$

where Q_m and Q_n are the adsorption amount of MIPs for the template molecule and analogues, respectively.

2.7 Desorption and enrichment of RhB

The RhB-adsorbed MIPs was firstly treated by centrifugation and drying at 60 ℃ under vacuum, and then re-suspended in distilled water or methanol/acetic acid (9:1, v/v) with a solid to liquid ratio of 20 mg/1 mL, followed by incubation in water bath at a certain temperature with continuous stirring for 24 h. The obtained mixture solution was centrifuged and the concentration of RhB in the supernatant was determined by UV/vis spectrometer. The desorption process was repeated four times, and the final product was washed with water and then dried under vacuum for recycling.

3 Results and Discussion

3.1 Characterization of LDH, modified-LDH samples, MIPs and corresponding NIPs

To determine the phase composition and crystal structure of the LDH, LDH-SDS, and LDH-SDS-Br, they were characterized by XRD analysis (Figure 1 and Figure 2a). The three typical basal reflections planes (003), (006), (009) indicated that the as-prepared LDH had a well-crystallized hydrotalcite-like structure (Figure 2a). The interlayer distance was calculated to be ca. 0.78 nm according to the (003) diffraction peak at 11.33°. However, after the anion exchange reaction of LDH with SDS and α-bromobutyrate, the diffraction peaks of LDH were obviously shifted to the low angles. The interlayer distances of LDH-SDS and LDH-SDS-Br were about 2.70 nm and 2.59 nm, respectively. Both of the interlayer distances were larger than that of the LDH, which was attributed to the intercalation of SDS^- and α-bromobutyrate by anion exchange. Moreover, basal spacing of the LDH-SDS (2.70 nm) was a bit larger than that of the LDH-SDS-Br (2.59 nm), indicating that the longer SDS^- anions chains were substituted partly with the shorter chains of α-bromobutyrate anions. The results suggested that the ATRP initiator (LDH-SDS-Br) was synthesized successfully.

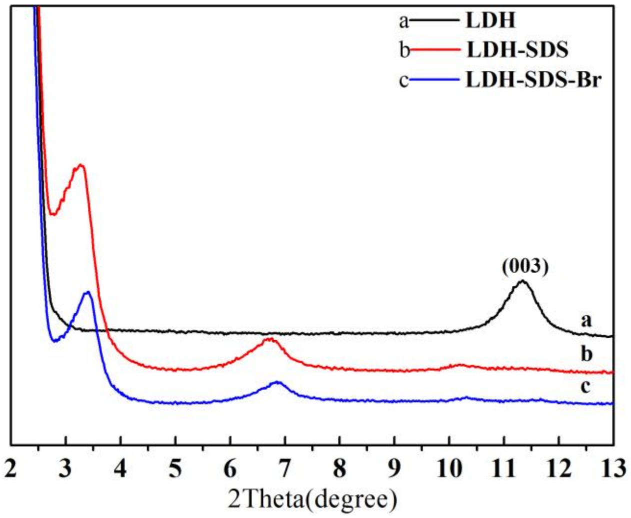

Figure 1. XRD patterns for the (a) LDH, (b) LDH-SDS and (c) LDH-SDS-Br.

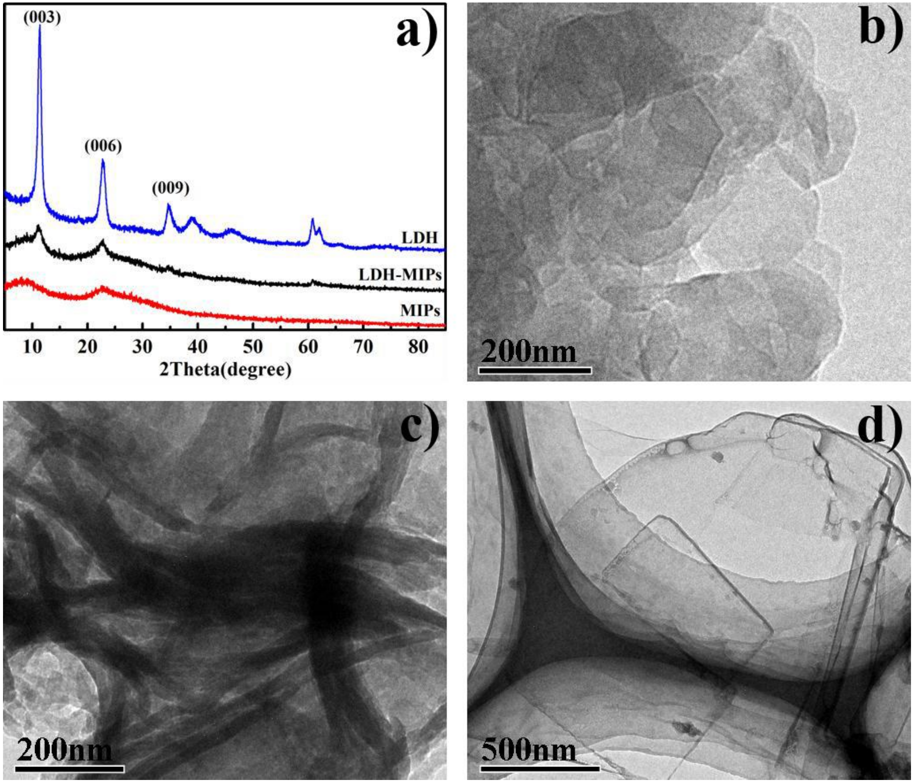

Figure 2. (a) XRD patterns and TEM images of (b) LDH, (c) LDH-MIPs, and (d) MIPs.

The membrane-structure MIPs were prepared by an ATRP method, using LDH-SDS-Br as the initiator. XRD analysis and TEM observation were performed to characterize the obtained materials. As shown in Figure 2a, after the ATRP reaction, the basic structure of LDH was retained in the LDH-MIPs, but these diffraction peaks were wider and less intense than that of the LDH, which was likely due to the existence of amorphous substance and the enlarged layers of the LDH. This was evidenced by the irregular morphology substances observed in the TEM image of LDH-MIPs (Figure 2c), which was not existed in the LDH structure (Figure 2b). Moreover, from the XRD patterns (Figure 2a), the obtained MIPs displayed an amorphous structure. As a result, it could be determined that the substance with an irregular morphology in LDH-MIPs was MIPs. Since LDH structure was not seen in the XRD patterns of MIPs (Figure 2a) and TEM image (Figure 2d), this suggested that the template substrate (LDH) could be removed completely by washing with methanol/acetic acid (9:1, v/v), which was also evidenced by the EDS spectra (Figure S1). In addition, the MIPs presented a membrane structure (Figure 2d), with a monolayer membrane thickness of about 1 nm according to the AFM characterization (Figure S2). It suggested that the ultra-thin membrane structural MIPs were prepared successfully by ATRP method with LDH as the template substrate.

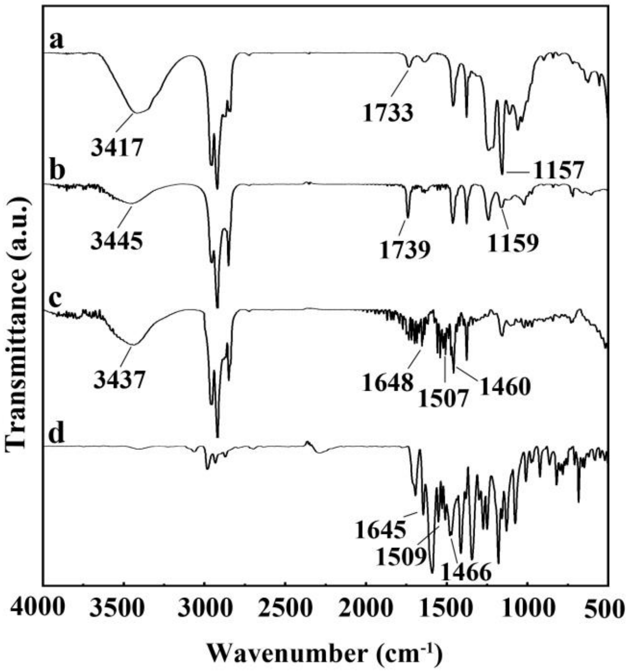

Figure 3. FTIR spectra of (a) NIPs, (b) MIPs, (c) RhB-absorbed MIPs, (d) RhB.

As a proof-of-concept study, RhB imprinted ultra-thin MIPs membranes were synthesized and used for the treatment of RhB in water. FTIR spectra were utilized to monitor the structural changes of the MIPs before and after adsorption. As shown in Figure 3b, characteristic peaks at 3445 cm^{-1} and 1739 cm^{-1} were assigned to the stretching vibration of –OH and C=O of MAA, respectively. A typical peak of C-O-C of EGDMA at 1159 cm^{-1} could also be seen[36]. There were not different characteristic peaks between MIPs and NIPs from the FTIR spectra (Figure 3b and Figure 3a), which indicated that MIPs without RhB could be acquired successfully by washing and the composition was similar to that of the NIPs. In the case of RhB, the apparent characteristic vibration peaks of benzene ring were observed at 1645 cm^{-1}, 1509 cm^{-1} and 1466 cm^{-1}. Those characteristic peaks of RhB could be found in the FTIR spectra of RhB-adsorbed MIPs (Figure 3c), which confirmed that RhB could be successfully adsorbed by MIPs. Additionally, the peak of –OH was shifting from 3445 cm^{-1} to 3437 cm^{-1}, which suggested that the binding between RhB and MAA was formed by hydrogen bonding[37].

3.2 Adsorption studies of MIPs and corresponding NIPs

The influence of temperature on RhB adsorption by MIPs is shown in Figure 4. It can be seen that the adsorption capacity of MIPs increased rapidly at first and then decreased gradually with temperature increasing. At the temperature of 25 ℃, the maximum adsorption capacity was obtained. This interesting phenomenon has also been reported in previous study[38-41]. The changes of adsorption capacity with temperature may be explained by many factors, such as change of pore size[42, 43], hydrophobic interaction[44], hydrogen-bond interaction[45], and so on. In order to study the influence of temperature on the pore size of polymers, we performed the BET measurements at 78 K and 88 K, respectively. There is a clear tendency that the pore size of the polymers increased as the temperature increased (Figure S3). Thus, pore size may be an important factor for the increase of adsorption capacity with temperature rising from 20 ℃ to 25 ℃, which facilitate the accession of RhB molecules to the specific cavities. However, hydrogen bonds between RhB molecules and binding sites could be destroyed by the rapid molecular motion in solution, which increased with temperature continuous rising, resulting in the weaker adsorption ability of the MIPs at high temperature. As a result, an optimal temperature of 25 ℃ was selected in the following adsorption reaction. Moreover, as the adsorption of MIPs for RhB was highly temperature-sensitive, this property can be employed as a desorption method, as discussed later.

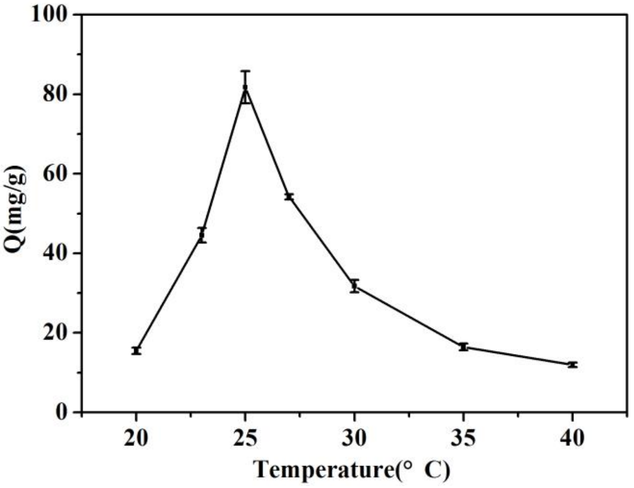

Figure 4. Effect of temperature on the adsorption capacity of MIPs. RhB initial concentration: 0.1 mM, volume: 2 mL, MIPs: 1 mg, adsorption time: 24 h. Each data point represents mean value of three measurements.

Figure 5 shows the binding isotherms of RhB onto MIPs and corresponding NIPs. The binding experiments were performed with different initial concentrations of RhB ranging from 1 μM to 1 mM. As seen in Figure 5, the adsorption amount of RhB onto MIPs and NIPs increased quickly with RhB concentration increased from 1 μM to 0.2 mM, and reached equilibrium over 0.2 mM. Compared to NIPs, the adsorption capacity of MIPs was obviously higher, with an α value of 1.76, which was also supported by the BET measurement of the MIPs and NIPs (111.9 m^2/g for MIPs, and 66.9 m^2/g for NIPs). It is suggested that specific recognition cavities for RhB were formed during the imprinting procedure so that the MIPs showed higher affinity and adsorption amount towards RhB than NIPs.

In addition, the binding behaviors of MIPs and NIPs were further evaluated by using the Langmuir (equation 1) and Freundlich (equation 2) isotherm models and the fitting results were obtained (Table S1). It can be seen that the Langmuir model had a better fit than the Freundlich model.

$$1/Q_e = 1/Q_{max} + 1/(bC_eQ_{max}) \quad (1)$$

$$\log Q_e = \log k + (1/n)\log C_e \quad (2)$$

where Q_e is the adsorption amount at equilibrium (mg/g), C_e is the equilibrium concentration (mg/L), Q_{max} is the maximum amount (mg/g) and b is the adsorption equilibrium constant (L/mg), k is the Freundlich constant (mg/g), and 1/n is the heterogeneity factor. The Q_{max} value obtained by the Langmuir model was 100.1 mg/g for MIPs, which was much higher than that of NIPs (60.4 mg/g). Compared with previously reported MIPs with other structures[46-50], the membrane structural MIPs presented a much higher adsorption amount and a slightly higher BET value. The result indicated that the membrane structural MIPs have large surface area that can locate more binding sites, which are more accessible than that of the bulk polymers.

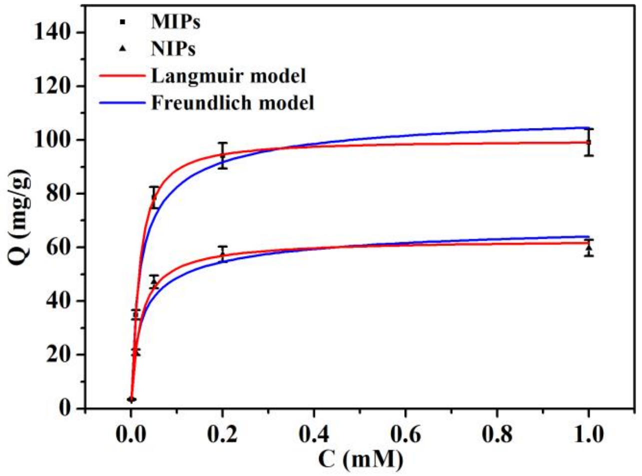

Figure 5. Langmuir and Freundlich isotherms for RhB adsorption on the MIPs and NIPs. MIPs or NIPs: 1 mg, volume: 4 mL, adsorption time: 24 h, temperature: 25 ℃. Each data point represents mean value of three measurements.

The adsorption kinetic experiments were conducted with the adsorption time varying from 0 to 36 h and the results were presented in Figure 6. Adsorption amounts of both the MIPs and NIPs increased rapidly and then slowed down in 13 h. The adsorption equilibrium was reached after 20-hour adsorption. Moreover, the adsorption capacity of MIPs was higher than that of the NIPs, which was attributed to the specific recognition cavities within the MIPs that displayed high affinity towards template molecule RhB. Meanwhile, different kinetic models including the pseudo-first-order, pseudo-second-order and intraparticle diffusion kinetic model were adopted to investigate the mechanism and rate-controlling step in the overall adsorption process, and the fitting results were presented in Table 1. The pseudo-first-order, pseudo-second-order and intraparticle diffusion kinetic models expressed by the following equations, respectively:

$$\ln(Q_e - Q_t) = \ln(Q_e) - k_1 t \quad (3)$$

$$\frac{t}{Q_t} = \frac{1}{k_2 Q_e^2} + \frac{t}{Q_e} \quad (4)$$

$$Q_t = k_{id} t^{1/2} + C \quad (5)$$

where Q_e and Q_t are the adsorption capacity at equilibrium and time t, respectively. k_1 is the rate constant of pseudo-first-order adsorption. k_2 is the rate constant of pseudo-second-order adsorption model. k_{id} indicates the intraparticle diffusion rate constant, and C provides information about the thickness of the boundary layer. As seen in Table 1, the results indicated that the adsorption process can be best fit by the pseudo second-order model (Figure 7), suggesting that the rate-limiting step may be the chemical sorption or chemisorption involving valency forces through sharing or exchange of electrons between the MIPs and the template molecule[51].

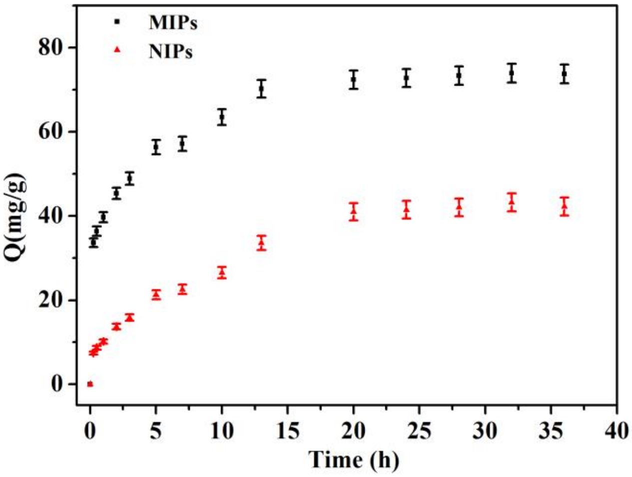

Figure 6. Adsorption kinetics of RhB on MIPs and NIPs. MIPs or NIPs: 5 mg, RhB concentration: 0.025 mM, volume: 100 mL, temperature: 25 ℃. Each data point represents mean value of three measurements.

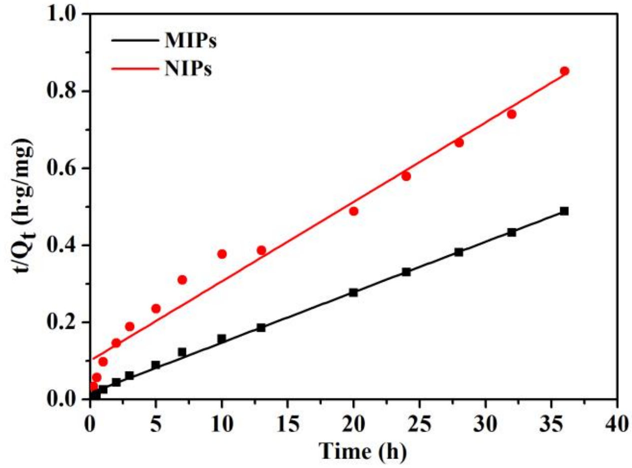

Figure 7. The pseudo-second-order kinetic model for the adsorption of RhB on MIPs and NIPs. MIPs or NIPs: 5 mg, RhB concentration: 0.025 mM, volume: 100 mL, temperature: 25 ℃.

Table 1. Parameters of different kinetic models for RhB adsorption on the MIPs and corresponding NIPs

Sorbents	^{a}Qe,exp	Pseudo-first-order			Pseudo-second-order			Intraparticle diffusion		
		k_1 (h^{-1})	$^{b}Q_e$ (mg g^{-1})	R^2	k_2 (g mg^{-1} h^{-1})	$^{b}Q_e$ (mg g^{-1})	R^2	k_{id} (mg g^{-1} $h^{-1/2}$)	C (mg g^{-1})	R^2
MIPs	73.77	1.0404	66.17	0.7813	0.0155	75.87	0.9975	9.3721	23.01	0.7918
NIPs	42.25	1.1304	42.78	0.9339	0.0055	46.51	0.9745	7.1637	4.26	0.9695

$^{a}Q_{e,exp}$ and $^{b}Q_e$ are the experimental value and the calculated value of the amount of RhB adsorbed on MIPs and NIPs at equilibrium (mg g^{-1}), respectively.

3.3 Binding specificity

Selectivity of the MIPs was evaluated by the adsorption experiment using a mixture solution of three dyes including Rhodamine B (RhB), Butyl Rhodamine B (BRhB) and Rhodamine 6G (Rh6G) (Figure 8). The concentration of each dye was 0.1 mM. As shown in Figure 8, the MIPs exhibited higher adsorption capacity for RhB than its analogs. The selectivity coefficients (β) of MIPs were calculated to be 22.57 (for RhB/BRhB) and 8.79 (for RhB/Rh6G), respectively (Table 2). It is suggested that specific artificial recognition cavities were introduced into the MIPs during the ATRP procedure, which were highly complementary to the template molecules. The high selectivity displayed by the membrane structure MIPs implied that this material was very suitable for selective preconcentration of dyes.

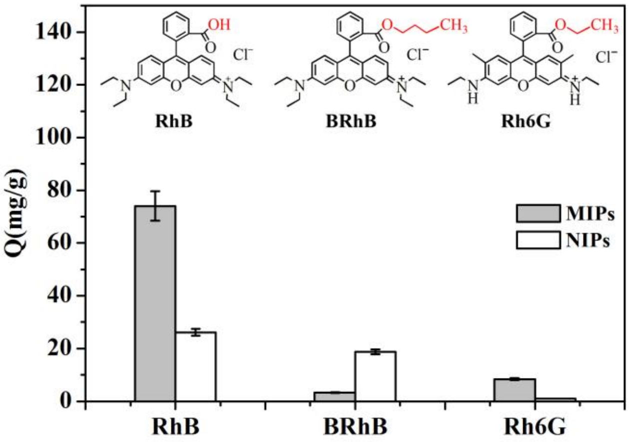

Figure 8. Binding capacities of three different dyes on MIPs and NIPs. MIPs or NIPs: 1 mg, volume: 4 mL, adsorption time: 24 h, temperature: 25 ℃. Each data point represents mean value of three measurements.

Table 2. Imprinting factors (α) and Selectivity (β) of MIPs and NIPs

target molecule[a]	Q_{MIPs}	Q_{NIPs}	α	β
RhB	74.03	26.12	2.83	—
BRhB	3.28	18.73	—	22.57
Rh6G	8.42	1.00	—	8.79

[a]The initial concentration of 0.1 mM for each target molecule in the mixed solution.

3.4 Desorption and enrichment of RhB

Desorption conditions of the MIPs were studied after RhB adsorption. Table 3 shows the RhB desorption efficiency and enrichment multiples using two desorption methods. When eluted with a mixture solution of methanol and acetic acid (9:1, v/v), the RhB was concentrated about 27.3 times for the first cycle and the desorption efficiency was calculated to be 93.4% after four continuous cycles. Additionally, as the adsorption of RhB was highly temperature-sensitive, a simple strategy was adopted to desorb the RhB just by changing the operating temperature. As presented in Table 3, at the temperature of 20 ℃, an enrichment multiple of 2.6 times was obtained in the first cycle, with a desorption efficiency of 25.7% after four continuous cycles, Similar enrichment multiple and desorption efficiency were also obtained at 40 ℃. Therefore, the temperature for desorption of dye can be chose according to the ambient temperature so that less energy is needed. Although the efficiency of desorption and enrichment was still unsatisfied, it provided a new strategy for dyes recycling, which was totally environmental-friendly and especially suitable for the reuse of dyes in textile industries. Moreover, as the thermosensitivity of MIPs is closely related to the pore structure, it may be possible to improve the efficiency by adjusting the ratio of function monomer, crosslinking agent and template molecules[38], which will be discussed in a future paper.

Table 3. RhB desorption efficiency and the enrichment multiples after desorbing RhB-adsorbed MIPs by different methods

	methods of desorption		
	Temperature control		Eluting method
	20 ℃	40 ℃	
MIPs dosage (g/L)	0.5	0.5	0.5
initial RhB concentration (mg/L)	20	20	20
desorption ratio (%) after one cycle	6.5	7.0	68.3
desorption ratio (%) after four cycles	25.7	27.1	93.4
enrichment multiples	2.6	2.8	27.3

3.5 Regeneration and reproducibility

As important aspects for an adsorbent, regeneration and reproducibility of the MIPs were assessed. Five desorption-reproducibility cycles were implemented by using the same MIPs and NIPs. As shown in Figure 9, the adsorption performance remained stable after five cycles with only 5% decrease of the maximum adsorption amount. There may be two possible reasons for the decrease of adsorption amount. On the one hand, a few recognition cavities within MIPs were damaged after repeated washing with the eluent. On the other hand, a bit of RhB molecules bound to the recognition cavities were not desorbed. As a result, a small number of recognition cavities could not match to template molecules any longer. But above all, the adsorption amount of MIPs was still higher than that of NIPs and the α reached up to 1.97 after five cycles.

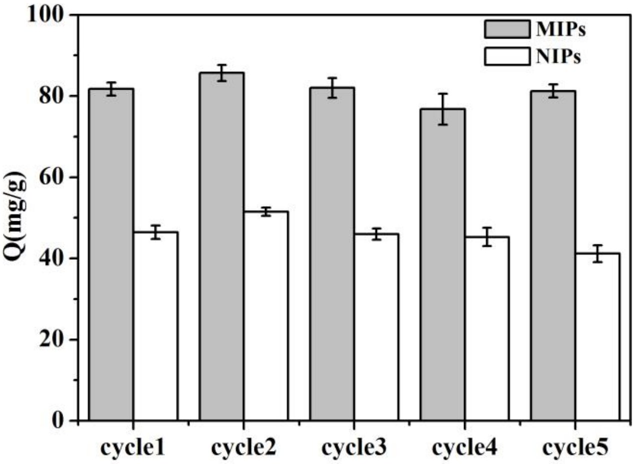

Figure 9. Regeneration and reproducibility of the MIPs and NIPs for five cycles. MIPs or NIPs: 1 mg, volume: 4 mL, adsorption time: 24 h, temperature: 25 ℃. Each data point represents mean value of three measurements.

3.6 Real sample analysis

Applicability of the MIPs for real water sample treatment was demonstrated by recovering RhB from RhB spiked lake water. The lake water was from XiHu Park (Fuzhou, Fujian province, China) and used without any pretreatment. The recovery experiments were explored using RhB spiked water at different concentration levels (0.5, 1.0 and 5.0 mg/L). As shown in Table 4, all the recovery ratios were greater than 90%, which suggested that the prepared MIPs was a promising adsorbent for the advanced treatment of dye wastewater.

Table 4. Recovery RhB spiked into lake water by MIPs[a]

Sample	RhB added (mg/L)	RhB adsorbed (mg/L)	Recovery (%)
Lake water	0.5	0.46 ± 0.01	92
	1.0	0.91 ± 0.01	91
	5.0	4.65 ± 0.06	93

[a] MIPs: 1 mg, volume: 2 mL, adsorption time: 24 h, at room temperature, n = 3.

4 Conclusions

In summary, an ultra-thin MIPs membrane with a thickness of 1 nm was synthesized via an ATRP method using LDH as the template substrate. Properties of the MIPs were characterized by XRD, TEM, AFM, FTIR and BET measurement. This material was applied for the selective adsorption of RhB in solution. Adsorption behaviors of the MIPs were studied and a high adsorption capacity of 100.1 mg/g was obtained. The enrichment of RhB at the level of 27.3 times was satisfied using acidic eluent. In the meanwhile, a simple and environmental-friendly desorption method was developed by changing the operating temperature. Moreover, the MIPs were highly selective and reproductive. Applicability of the material was demonstrated by the recovering of RhB in spiked lake water. This membrane-structure MIPs is a promising adsorbent for the treatment of dyes wastewater and recycling of organic resources in wastewater.

Acknowledgements

This work was financially supported by the National Basic Research Program of China (2014CB932101,2013CB934302), the Outstanding Youth Fund (21125730), the National Science Foundation Grant (21307130), the "Strategic Priority Research Program" of the Chinese Academy of Sciences (XDA09030203).

Notes and references

[a] College of Chemistry, Fuzhou University, Fuzhou, Fujian 350002, China.
[b] Key Laboratory of Optoelectronic Materials Chemistry and Physics, Fujian Institute of Research on the Structure of Matter, Chinese Academy of Sciences, Fuzhou, Fujian 350002, China.
[c] Key Laboratory of Design and Assembly of Functional Nanostructures, Fujian Institute of Research on the Structure of Matter, Chinese Academy of Sciences, Fuzhou, Fujian 350002, China. E-mail: btzhang@fjirsm.ac.cn; zlin@fjirsm.ac.cn; Tel: +86-591-83705474; Fax: +86-591-83705474
[d] School of Environment and Energy, South China University of Technology, Guangzhou 510006, China.

1 X. Luo, Y. Zhan, Y. Huang, L. Yang, X. Tu and S. Luo, *J. Hazard. Mater.*, 2011, 187, 274-282.
2 J. T. Spadaro, L. Isabelle and V. Renganathan, *Environ. Sci. Technol.*, 1994, 28, 1389-1393.
3 N. Daneshvar, H. Ashassi-Sorkhabi and A. Tizpar, *Sep. Purif. Technol.*, 2003, 31, 153-162.
4 J. Sarasa, M. P. Roche, M. P. Ormad, E. Gimeno, A. Puig and J. L. Ovelleiro, *Water Res.*, 1998, 32, 2721-2727.
5 S. H. Lin and C. F. Peng, *Water Res.*, 1996, 30, 587-592.
6 S. Cheng, D. L. Oatley, P. M. Williams and C. J. Wright, *Water Res.*, 2012, 46, 33-42.
7 F. I. Hai, K. Yamamoto, F. Nakajima and K. Fukushi, *Water Res.*, 2011, 45, 2199-2206.
8 A. Pandey, P. Singh and L. Iyengar, *Int. Biodeter. Biodegr.*, 2007, 59, 73-84.
9 M. Riera-Torres, C. Gutiérrez-Bouzán and M. Crespi, *Desalination*, 2010, 252, 53-59.
10 Y. Al-Degs, M. A. M. Khraisheh, S. J. Allen, M. N. Ahmad and G. M. Walker, *Chem. Eng. J.*, 2007, 128, 163-167.
11 P. Baskaralingam, M. Pulikesi, D. Elango, V. Ramamurthi and S. Sivanesan, *J. Hazard. Mater.*, 2006, 128, 138-144.
12 G. Z. Kyzas, N. K. Lazaridis and A. C. Mitropoulos, *Chem. Eng. J.*, 2012, 189-190, 148-159.
13 Y. Wang, J. Chen, L. Lu and Z. Lin, *ACS appl. mater. interfaces*, 2013, 5, 7698-7703.
14 Y. Wang, D. Chen, Y. Wang, F. Huang, Q. Hu and Z. Lin, *Nanoscale*, 2012, 4, 3665-3668.
15 S. Piletsky and A. P. Turner, *Molecular imprinting of polymers*, Landes Bioscience Georgetown, TX, USA, 2006.
16 L. Chen, S. Xu and J. Li, *Chem. Soc. Rev.*, 2011, 40, 2922-2942.
17 W. Chen, W. Lei, M. Xue, F. Xue, Z.-h. Meng, W.-b. Zhang, F. Qu and K. J. Shea, *J. Materi. Chem. A*, 2014, 2, 7165.
18 R. N. Liang, D. A. Song, R. M. Zhang and W. Qin, *Angew. Chem. Int. Ed. Engl.*, 2010, 49, 2556-2559.
19 D. Y. Li, X. W. He, Y. Chen, W. Y. Li and Y. K. Zhang, *ACS appl. mater. interfaces*, 2013, 5, 12609-12616.
20 B. Rezaei, O. Rahmanian and A. A. Ensafi, *Sensor.Actuat. B-Chem.*, 2014, 196, 539-545.
21 H.-H. Yang, S.-Q. Zhang, W. Yang, X.-L. Chen, Z.-X. Zhuang,

J.-G. Xu and X.-R. Wang, *J. Am. Chem. Soc.*, 2004, 126, 4054-4055.
22 Z. Lin, Z. Xia, J. Zheng, D. Zheng, L. Zhang, H. Yang and G. Chen, *J. Mater. Chem.*, 2012, 22, 17914.
23 J. Luo, S. Jiang and X. Liu, *J. Phys. Chem. C*, 2013, 117, 18448-18456.
24 G. Z. Kyzas, N. K. Lazaridis and D. N. Bikiaris, *Carbohydr. Polym.*, 2013, 91, 198-208.
25 G. Z. Kyzas, D. N. Bikiaris and N. K. Lazaridis, *Chem. Eng. J.*, 2009, 149, 263-272.
26 Y. Li, X. Li, J. Chu, C. Dong, J. Qi and Y. Yuan, *Environ. Pollut.*, 2010, 158, 2317-2323.
27 X. Yang, Z. Zhang, J. Li, X. Chen, M. Zhang, L. Luo and S. Yao, *Food Chem.*, 2014, 145, 687-693.
28 H. Zhang, Z. Zhang, Y. Hu, X. Yang and S. Yao, *J. Agric. Food. Chem.*, 2011, 59, 1063-1071.
29 M. R. Halhalli, C. S. A. Aureliano, E. Schillinger, C. Sulitzky, M. M. Titirici and B. Sellergren, *Poly. Chem.*, 2012, 3, 1033.
30 E. Yildirim, E. Turan and T. Caykara, *J. Mater. Chem.*, 2012, 22, 636.
31 D. Yin and M. Ulbricht, *Biomacromolecules*, 2013, 14, 4489-4496.
32 H.-J. Wang, W.-H. Zhou, X.-F. Yin, Z.-X. Zhuang, H.-H. Yang and X.-R. Wang, *J. Am. Chem. Soc.*, 2006, 128, 15954-15955.
33 P. Ding, Z. Li, S. Tang, N. Song and L. Shi, *Microchimica. Acta.*, 2013, 180, 599-605.
34 Y. Li, B. Gao, T. Wu, D. Sun, X. Li, B. Wang and F. Lu, *Water Res.*, 2009, 43, 3067-3075.
35 L. Qiu, W. Chen and B. Qu, *Colloid. Polym. Sci.*, 2005, 283, 1241-1245.
36 X. Cai, J. Li, Z. Zhang, F. Yang, R. Dong and L. Chen, *ACS appl. mater. interfaces*, 2014, 6, 305-313.
37 H. Ebrahimzadeh, Z. Dehghani, A. A. Asgharinezhad, N. Shekari and K. Molaei, *Int. J. Pharm.*, 2013, 453, 601-609.
38 L. Qin, X. He, W. Zhang, W. Li and Y. Zhang, *Anal. Chem.*, 2009, 81, 7206-7216.
39 F.-X. Gao, X.-L. Zhao, X.-W. He, W.-Y. Li and Y.-K. Zhang, *Anal. Methods*, 2013, 5, 6700.
40 J. Pan, H. Hang, X. Li, W. Zhu, M. Meng, X. Dai, J. Dai and Y. Yan, *Appl. Surf. Sci.*, 2013, 287, 211-217.
41 N. Li, L. Qi, Y. Shen, J. Qiao and Y. Chen, *ACS appl. mater. interfaces*, 2014, 6, 17289-17295.
42 A. Saeed, M. Sharif and M. Iqbal, *J. Hazard. Mater.*, 2010, 179, 564-572.
43 M. Zabihi, A. Haghighi Asl and A. Ahmadpour, *J. Hazard. Mater.*, 2010, 174, 251-256.
44 L. Uzuna, R. Sayb, S. Ünalc and A. Denizli, *J. Chromatogr. B*, 2009, 877, 181-188.
45 Y. Tao, J. Dai, Y. Kong and Y. Sha, *Anal. Chem.*, 2014, 86, 2633-2639.
46 M. Gan, J. Pan, Y. Zhang, X. Dai, Y. Yin, Q. Qu and Y. Yan, *Chem. Eng. J.*, 2014, 257, 317-327.
47 F.-X. Gao, X.-T. Ma, X.-W. He, W.-Y. Li and Y.-K. Zhang, *Colloids Surf. A*, 2013, 433, 191-199.
48 Y. Wu, M. Yan, Y. Yan, X. Liu, M. Meng, P. Lv, J. Pan, P. Huo and C. Li, *Langmuir* , 2014, 30, 14789-14796.
49 X. Xie, X. Pan, S. Han and S. Wang, *Anal. bioanal. chem.*, 2015, DOI: 10.1007/s00216-014-8425-0.
50 T. Zhao, X. Guan, W. Tang, Y. Ma and H. Zhang, *Anal. Chim. Acta*, 2015, 853, 668-675.
51 M. G. Ho Y.S., *Process Biochem.*, 1999, 34, 451–465.

Template synthesized ultra-thin molecularly imprinted polymers membrane for selective preconcentration of dyes

Lili Lu,[a,b] Xianyang Yue,[b] Fuquan Lin,[a,c] Feng Huang,[b] Bintian Zhang*[c] and Zhang Lin*[c,d]

[a]College of Chemistry, Fuzhou University, Fuzhou, Fujian 350002, China.

[b]Key Laboratory of Optoelectronic Materials Chemistry and Physics, Fujian Institute of Research on the Structure of Matter, Chinese Academy of Sciences, Fuzhou, Fujian 350002, China.

[c]Key Laboratory of Design and Assembly of Functional Nanostructures, Fujian Institute of Research on the Structure of Matter, Chinese Academy of Sciences, Fuzhou, Fujian 350002, China. E-mail: btzhang@fjirsm.ac.cn; zlin@fjirsm.ac.cn; Tel: +86-591-83705474; Fax: +86-591-83705474

[d]School of Environment and Energy, South China University of Technology, Guangzhou 510006, China.

An ultra-thin molecularly imprinted polymers (MIPs) membrane was synthesized via surface imprinting technique using layered double hydroxides (LDH) as the template substrate and applied for the selective preconcentration of RhB in wastewater.